Wildfire emissions disrupt black carbon and $PM_{2.5}$ mortality burden trends across the continental US

Authors: Jing Wei[1,2*], Jun Wang[1*], Zhanqing Li[2], Shobha Kondragunta[3], Susan Anenberg[4], Yi Wang[1], Huanxin Zhang[1], David Diner[5], Jenny Hand[6], Alexei Lyapustin[7], Ralph Kahn[7], Peter Colarco[8], Arlindo da Silva[9], Charles Ichoku[10]

Affiliations:

1. Department of Chemical and Biochemical Engineering, Iowa Technology Institute, Center for Global and Regional Environmental Research, University of Iowa, Iowa City, IA 52242, USA
2. Department of Atmospheric and Oceanic Science, Earth System Science Interdisciplinary Center, University of Maryland, College Park, MD 20472, USA
3. Center for Satellite Applications and Research, NOAA/NESDIS, College Park, MD 20740, USA
4. Department of Environmental and Occupational Health, George Washington University, Washington, DC 20052, USA
5. Jet Propulsion Laboratory, California Institute of Technology, Pasadena, CA 91109, USA
6. Cooperative Institute for Research in the Atmosphere, Colorado State University, Fort Collins, CO 80523, USA
7. Climate and Radiation Laboratory, NASA Goddard Space Flight Center (GSFC), Greenbelt, MD 20771, USA
8. Atmospheric Chemistry and Dynamics Laboratory, NASA GSFC, Greenbelt, MD 20771, USA
9. Global Modeling and Assimilation Office, NASA GSFC, Greenbelt, MD 20771, USA
10. College of Arts & Sciences, Howard University, Washington, DC 20059, USA

*Corresponding authors: Jun Wang, jun-wang-1@uiowa.edu ; Jing Wei: jing-wei@uiowa.edu

Classification: Physical Science (major), Atmospheric (minor)

Keywords: fine particulate matter, black carbon, wildfires, mortality burden, deep learning

Abstract (< 250 words, currently 250)

The long-term improvement trends in air quality and public health in the continental United States (US) were obscured in the past decade by the increase of fire emissions that potentially counterbalanced the decline in anthropogenic emissions. Here, we estimate daily concentrations of fine particulate matter ($PM_{2.5}$) and its highly toxic component, black carbon (BC), at 1 km resolution in the US from 2000 to 2020 via deep learning that integrates big data from satellites, models, and surface observations. Daily (monthly) $PM_{2.5}$ and BC estimates are reliable with cross-validated R^2 values of 0.85 (0.98) and 0.79 (0.94), respectively. Both $PM_{2.5}$ and BC in the US show overall decreasing trends of 23% and 18% over the past two decades, leading to a reduction in premature deaths by ~1800 [95% confidence interval (CI): 1300, 2300] people per year. However, the premature death trend has downshifted since 2010; the western US exhibits large interannual fluctuations caused by wildfires, leading to an increase in $PM_{2.5}$ concentrations and associated deaths [~360 (95% CI: [230, 510]) people] per year. In contrast, removing years with large fires would lead to a more significant decreasing trend in $PM_{2.5}$ concentrations. Furthermore, the BC-to-$PM_{2.5}$ mass ratio for the US as a whole shows a significant increase of 1.82% per year, primarily due to the reduction of inorganic emissions and suggesting a potential increase in relative toxicity of $PM_{2.5}$. Reducing fire risk via effective policies including mitigation of climate warming can substantially improve air quality and public health in the coming decades.

Main text

Atmospheric particulate matter (PM) with an aerodynamic diameter of ≤ 2.5 μm ($PM_{2.5}$) has significant impacts on air quality, climate change, and public health (1, 2). Understanding and estimating these impacts requires knowledge of the spatiotemporal variations of the amount and composition of surface-level $PM_{2.5}$, but it is challenging due to multiple factors, including the change in and diversity of aerosol sources and aerosol processes as well as the limited number of surface observation sites. Anthropogenic sources are being regulated in many countries, whereas wildfires show significant temporal variations; both are significant contributors to the $PM_{2.5}$ mass and composition, including sulfate, nitrate, ammonium, organic carbon, and black carbon (BC). Of particular importance is BC, due to its strong absorption of solar radiation and consequent warming effect on climate (3, 4) as well as its high toxicity and hence potentially more severe impact on public health (5-9). However, even in the United States (US), where the history records of anthropogenic emissions are well documented, the national outcome of reduced emissions on public health associated with $PM_{2.5}$ and BC exposure still has not been studied on decadal scales (Table S1). Public health outcomes are obscured by large annual fluctuations in fire emissions and associated uncertainties regionally and seasonally. Only a few studies have shown the acute health effects (such as respiratory, cardiovascular, and asthma hospital admissions) from short-term exposure to increased ambient $PM_{2.5}$ and BC mass concentration associated with fire emissions (10-12).

How have the surface $PM_{2.5}$ mass and its fraction of BC changed in the past two decades in the continental US? And how much change (if any) in mortality burden due to $PM_{2.5}$ exposure may be attributed to fires? Here, we tackle both questions by building upon the advances enabled by machine learning (ML) and the long-term data record of aerosol measurements from both space and the surface over the US. Past studies have integrated satellite-based aerosol optical depth (AOD) products together with in situ ground measurements to estimate surface $PM_{2.5}$ over the US via approaches such as kriging (13), land-use regression modeling (14), neural network (15), random forest (16), geographically weighted regression (17), ML ensemble-based modeling (18), and convolutional neural network (19). Unlike $PM_{2.5}$, there are few studies focusing on BC estimates in the US (9, 17). The time periods of most previous studies are particularly short (< 10 years, Table S1). Although it has been postulated that the $PM_{2.5}$ concentration in the US should be

declining due to persistent regulations to reduce anthropogenic emissions since enaction of the Clean Air Act (CAA) of the 1970s, this conjecture cannot be fully verified with surface observation alone because it lacks full continental spatial coverage, especially when considering the recent increase of fires in the western US (20-23). As fire emissions are the second-largest source of BC in the US and a key source of $PM_{2.5}$ in fire-prone areas (24, 25), both the amount and the toxicity of ambient $PM_{2.5}$ could be increased, which leads to the hypothesis that the overall $PM_{2.5}$ impact on the public health burden may not change at all or might even have increased in the US in the past two decades, at least in the west.

We derived surface $PM_{2.5}$ and BC concentrations from 2000 to 2020 in the US with full spatial coverage via the deep learning (DL) approach and estimated the mortality burden in terms of the number of premature deaths associated with the change of $PM_{2.5}$ and BC at the national and regional scales. Our DL-based method integrates multiple sources of satellite-based data products, reanalysis datasets of aerosol composition, and datasets from surface monitoring stations in the US. Our method mitigates the impacts of the missing data associated with the spatial gaps in the satellite AOD retrievals due to clouds and surface snow or ice cover, and considers both spatial and temporal variations of the AOD-$PM_{2.5}$ relationship. Our long-term estimate of BC is made daily at 1 km resolution, in contrast with past studies that used chemical transport models at a much coarser resolution (50 km or larger) (9) and monthly or annual averages (17) (Table S1).

The association of health outcomes with exposure to $PM_{2.5}$ is often assessed by integrating $PM_{2.5}$ mass concentration and population density distribution with different concentration-response functions (CRFs), such as the Integrated Exposure–Response (IER) model (26). The IER model was defined by the Global Burden of Disease (GBD) 2017 study (27) and was further updated in the recent GBD 2019 study (28). Using the IER model, Apte et al. (29) illustrated that the emission reduction of global $PM_{2.5}$ to meet the World Health Organization guidance could have avoided 23% of the population deaths attributable to ambient $PM_{2.5}$ in 2010. However, the CRFs in the IER model are steeper in clean areas, suggesting higher sensitivity of the mortality burden to the change of $PM_{2.5}$ by fire emissions in the US than in more polluted countries (such as China or India). Wang et al. (30) found that, in California, the mortality burden in 2012 from exposure to air pollution that originated in nonlocal sources was greater than that caused by local anthropogenic emissions.

Aguilera et al. (31) found that the $PM_{2.5}$ generated from the wildfires had larger effects on the human respiratory system than $PM_{2.5}$ from other sources in Southern California during 1999–2012.

Although the mortality burden associated with $PM_{2.5}$ exposure has been estimated in many studies, few have investigated the health impacts of BC in the US (7-9, 32), which is due in part to the limited availability of both exposure data sources and CRF for BC. Smith et al. (32) calculated the mortality effects related to long-term BC exposure in 66 US cities through the cohort study. Pond et al. (7) and Wang et al. (8) documented two cohort studies showing the significant positive associations of cardiopulmonary and all-cause mortality, respectively, with exposure to major $PM_{2.5}$ components, especially BC, in the US. Li et al. (9) estimated ~14,000 premature deaths caused by ambient BC in 2010 in the US. Here, we study the long-term (2000–2020) mortality burden from exposure to both $PM_{2.5}$ and its BC component at each 1 km^2 grid in the continental US and investigate the role of fire emissions in changing the annual mortality burden since the start of the new millennium. For the mortality burden assessment, the CRF of $PM_{2.5}$ was collected from GBD 2019, and a sensitivity study was also conducted by taking the CRF of BC from the literature to consider the potentially greater toxicity of BC compared with other $PM_{2.5}$ components (see Materials and Methods).

Results and Discussion

Evaluation of $PM_{2.5}$ and BC predictions. The daily $PM_{2.5}$ and BC estimates at 1 km resolution in the continental US are evaluated via the widely used 10-fold cross-validation approach (33, 34). The DL-based approach works well in capturing daily surface $PM_{2.5}$ levels. At more than 82% and 79% of surface observation sites, cross-validation yields high R^2 (coefficient of determination) values greater than 0.7, and low values of normalized root mean square error (NRMSE) less than 0.4, respectively, especially for the eastern US (Fig. 1a). With a spatial distribution pattern similar to that of surface $PM_{2.5}$, surface BC estimates overall have slightly smaller R^2 values compared to ground-based observations (Fig. 1d), indicating a relatively decreasing accuracy in our estimates due to the much smaller concentration of BC and the relatively large uncertainty of BC measurements (a factor of two as compared to 10% for $PM_{2.5}$) (35, 36). For the 21-year study period in the US, all daily $PM_{2.5}$ and BC estimates show high fidelity, with average R^2 values of 0.85 and 0.79 against surface observations, and exhibit NRMSE values of 0.33 and 0.61,

respectively (Fig. 1a and 1d). These statistical agreements are further improved upon in the comparisons of monthly (i.e., CV-R^2 = 0.98 and 0.94, NRMSE = 0.08 and 0.26, Fig. 1b and 1e) and annual (i.e., CV-R^2 = 0.99 and 0.96, NRMSE = 0.05 and 0.16, Fig. 1c and 1f) averages. In addition, in terms of overall accuracy, our $PM_{2.5}$ and BC estimates are more reliable than or comparable to those in previous studies with reference to ground measurements on different temporal scales (Table S1) (14-19), which ensures that the exposure data of $PM_{2.5}$ and BC have the accuracy needed for assessing the effects of long-term $PM_{2.5}$ exposure on public health.

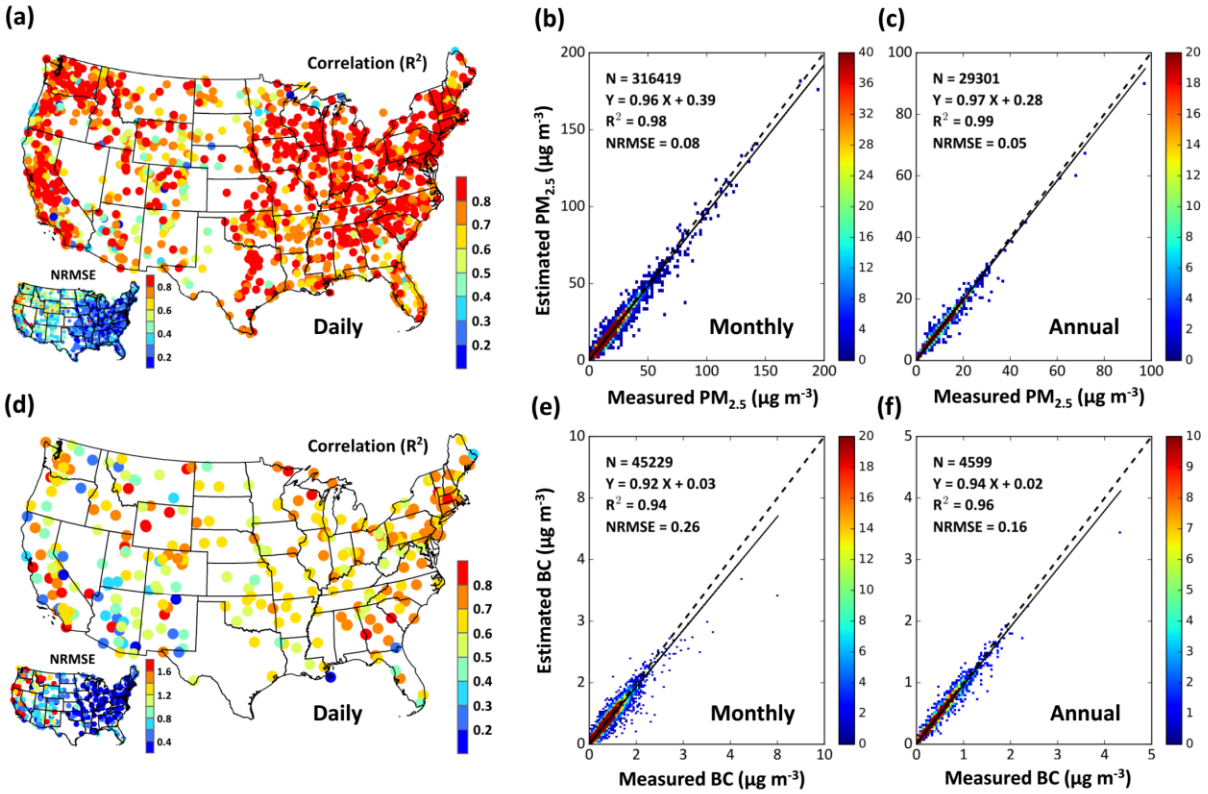

Fig. 1. Spatial distribution of R^2 in the cross-validation of daily (a) $PM_{2.5}$ and (d) BC estimates (unit: μg m^{-3}) at each ground monitoring station during the years 2000–2020 in the US. Also shown are the inter-comparison of measured (x-axis) and estimated (y-axis) of (b & e) monthly and (c & f) annual $PM_{2.5}$ (top row) and BC concentration (bottom row), respectively, in units of μg m^{-3}. The insets in (a) and (d) show the spatial distribution of normalized root mean square error (NRMSE).

Spatiotemporal variations of $PM_{2.5}$, BC, and mortality burden. Figure 2 shows the spatiotemporal distribution on average and the trend of $PM_{2.5}$, BC, and mortality burden in the US during the years 2000–2020 (maps for each year are provided in the Supplementary Information

(SI) in Figs. S1-S3). Both annual $PM_{2.5}$ and BC concentrations have similar spatial distributions; their mean values of 9.5 ± 2.0 μg m^{-3} and 0.44 ± 0.16 μg m^{-3} in the eastern US (EUS) are about 1.9 and 2.2 times higher than their counterparts in the western US except California (WUS, Fig. 2a, b) and 1.2 and 1.5 times higher than those in the central US (CUS), which reflects the population distribution and anthropogenic emissions. At the individual state level, the highest persistent pollution levels are found in some areas in California, likely reflecting the wildfire smoke patterns and local source of dust, especially in the central valley. Indeed, both $PM_{2.5}$ and BC increase by 35–38% in the fire seasons (autumn and summer) when compared to normal seasons (spring and winter) in the WUS (Figs. S4-S5). The cumulative number of premature deaths associated with exposure to $PM_{2.5}$ pollution in most parts of the US is relatively small because of the small population density in these areas. The total mortality burden in the continental US is estimated to be ~1.8 million (95% CI: [1.1, 2.6]) during the 21-year period of this study (Fig. 2c). As expected, these premature deaths were mainly concentrated in cities with large populations, such as Los Angeles, Houston, Chicago, Atlanta, and New York. In addition, our 1 km high-spatial-resolution data allows us to study air pollution and its impacts on public health at a much finer scale (see magnified images in Fig. 2). Large differences in the pollution levels of urban and rural regions can be clearly seen; in particular, high BC concentrations along highways due to traffic-related emissions (from diesel trucks) are well captured. In addition, contrasting distributions in the mortality burden in large cities and their surrounding areas can also be well characterized. These results highlight the unique advantages of high-resolution air pollution data.

Temporally, the annual amounts of $PM_{2.5}$ and BC in the years 2000–2020 show steadily declining trends in the EUS, remain nearly the same in the CUS (Fig. 2d-e), and fluctuate with large variations in sign and magnitude across the WUS. In the WUS, significant decreasing trends were observed in the city clusters located in the southwest (Los Angeles) and northwest (Seattle) corners; by contrast, significant increasing trends were found in most central inter-mountainous and northwest areas, especially Northern California and Oregon. At the seasonal scale, declining trends throughout the US were found in winter and spring; however, in summer and autumn, trends were opposite, increasing in the WUS and decreasing in the EUS (Fig. S6-S7), which suggests the increasing impacts of wildfires on surface $PM_{2.5}$ and BC, as these are the fire seasons in the WUS (37, 38). Overall, in the past two decades, the total number of premature deaths associated with

exposure to $PM_{2.5}$ has reduced (> 10^{-3} per km^2 per year) in populated parts of the US, especially in the EUS. It is also worthy to mention that this was also observed in places where $PM_{2.5}$ pollution go down, but population go up (Fig. S8), which was mainly contributed to the improved air quality. Regionally, an increased number of deaths is found only in a few large cities located in the western and southern US (Fig. 2f), which may be attributed to an increase in local fire and dust emissions (20, 23, 39), transboundary transport from Mexico (40, 41), and/or an increase in population density (Fig. S8).

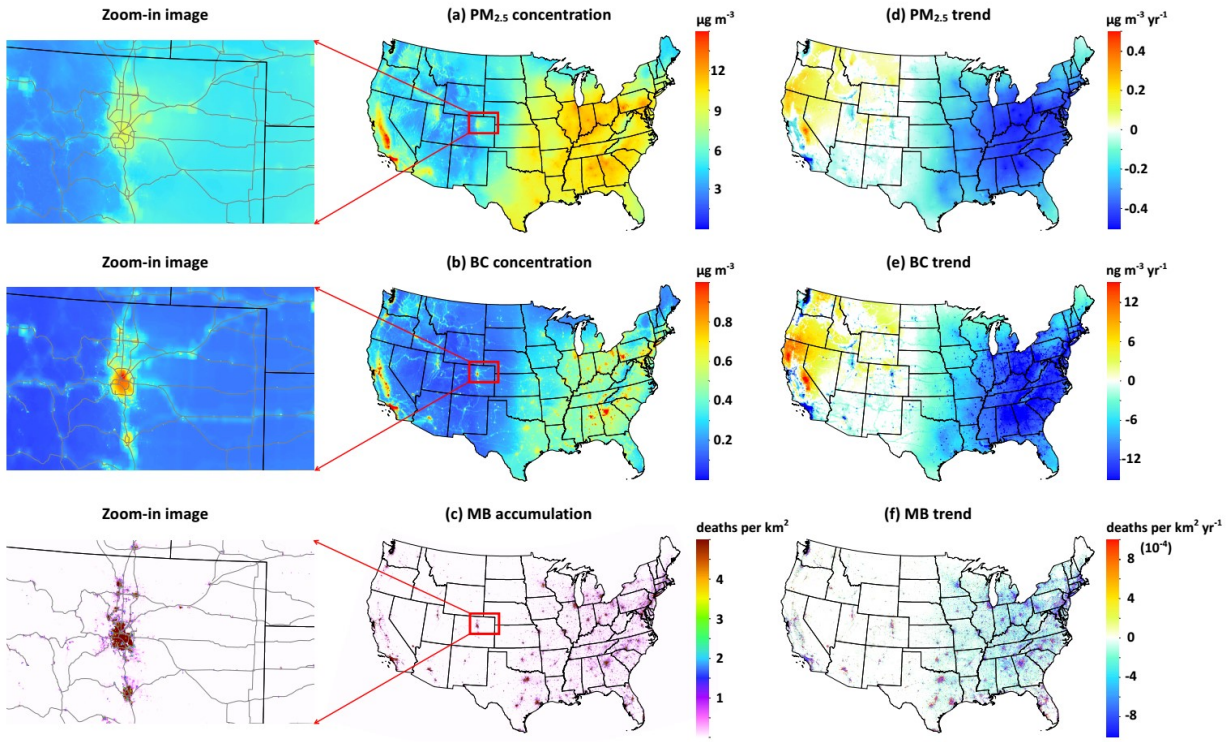

Fig. 2. Spatial distribution of the annual mean (a) $PM_{2.5}$ concentration (unit: μg m^{-3}), (b) BC concentration (unit: μg m^{-3}), (c) total cumulative mortality burden (MB) (unit: premature deaths per km^2) during the years 2000-2020 in the US, and zoomed-in images (left column) for the Denver area, in which the gray lines represent the roads, and (d-f) represent corresponding annual trends across the US. Only the trends that are significant at the 95% ($p < 0.05$) confidence level are shown.

The trends of the time series of annual mean $PM_{2.5}$, BC, and premature deaths during the years 2000–2020 were analyzed for the continental US, EUS, and WUS (Fig. 3). At the national level, $PM_{2.5}$ and BC concentrations overall declined by ~23% and 18% during the entire period, with the highest and lowest levels in 2000 and 2019, respectively. The decreasing trends were larger in the

first decade and slowed in the second decade (Fig. 3a, d). Looking geographically, greater declining trends of 49% and 43% with small fluctuations were seen in the EUS (42) (Fig. 3b, e), whereas in the WUS, virtually no trends existed during the entire period due to larger interannual fluctuations (Fig. 3c, f), particularly in summer and autumn (Fig. S9c, f). More importantly, significant downward trends ($p < 0.1$ and 0.05) were observed before 2010 but were then reversed (slope > 0), likely showing the impact of increasing fire emissions in recent years (as revealed in the analysis below).

The annual number of total premature deaths exposure to $PM_{2.5}$ pollution across the continental US first significantly decreased from 110 [95% confidence interval (CI): 71, 154] thousand in 2000 to 79 (95% CI: 50, 114) thousand in 2010; it then stabilized at nearly constant level with only small fluctuations (blue line in Fig. 3g). A continuous decrease in deaths at a significant rate of ~1260 people per year ($p < 0.01$) was observed in the EUS (blue line in Fig. 3h). In contrast, in the WUS (blue line in Fig. 3i), the annual death burden had a steady decrease (slope = -0.64 thousand per year, $p < 0.01$) until 2010 [16 thousand; 95% CI: (10, 24)], after which there was a significant increase (slope = 0.36 thousand per year, $p < 0.05$) with large annual fluctuations, leading to the peak burden in 2020 [22 thousand; 95% CI: (14, 32)].

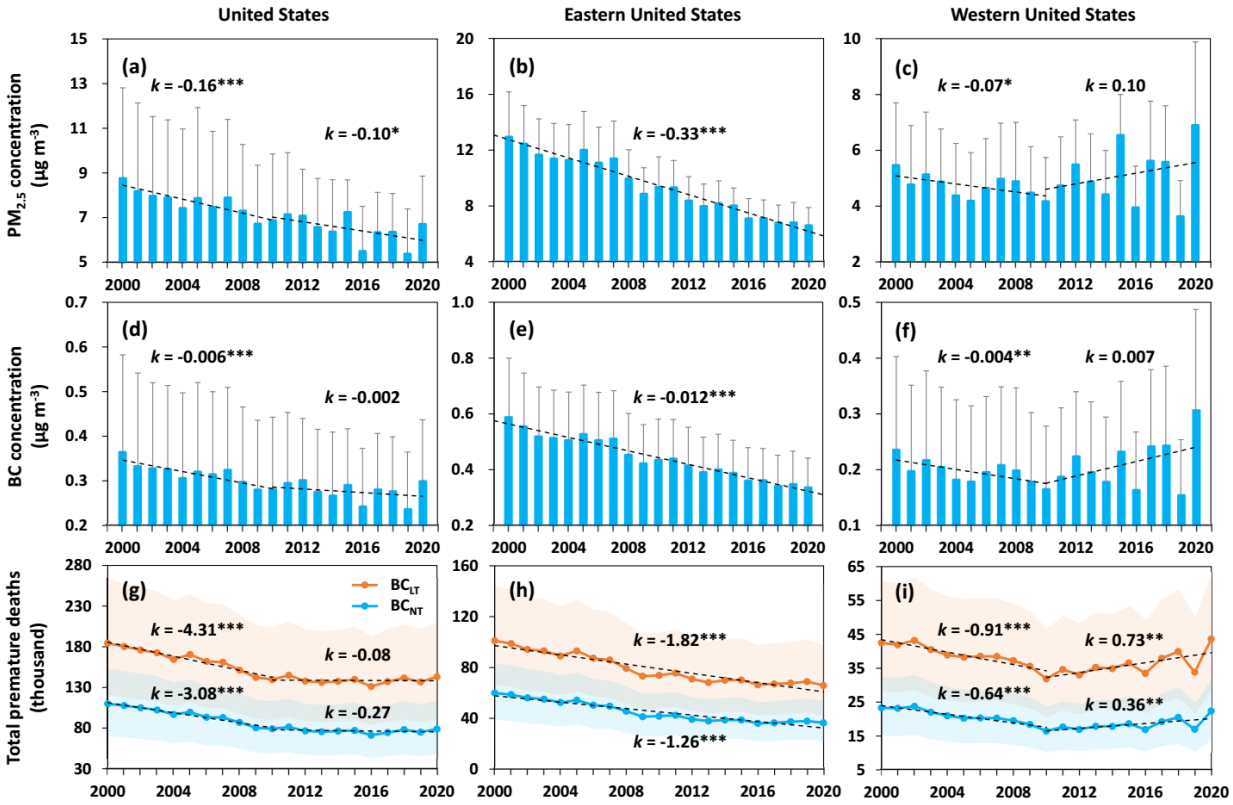

Fig. 3. Time series of annual and area mean of (a-c) $PM_{2.5}$ concentrations (μg m^{-3}), (d-f) BC concentrations (μg m^{-3}), and (g-i) total premature deaths (unit: thousand) associated with the total $PM_{2.5}$ pollution in the years 2000–2020 in the continental US, eastern US, and western US, respectively. Orange and blue lines denote the estimates of premature deaths with and without considering the larger toxicity of BC (BC_{LT} and BC_{NT}), respectively. The regression lines are shown as black dotted lines, and their slope (k) values are also given with *, **, and ***, representing trends that are significant at the 90% ($p < 0.1$), 95% ($p < 0.05$), and 99% ($p < 0.01$) confidence levels, respectively.

Impact of fire emissions and importance of BC on premature mortality. As more recent cohort studies have documented the importance of aerosol composition, especially BC, for the assessment of mortality burden, it is necessary to analyze not only the absolute amount but also the fractional concentration of BC. Figure 4 shows the spatiotemporal variations of BC-to-$PM_{2.5}$ ratio (BPR) in summer from 2000 to 2020. High BPR values of 5-10% are mainly distributed in major metropolitan areas (Seattle, San Francisco, Denver, etc.), consistent with the mass fraction of BC in anthropogenic emissions of $PM_{2.5}$ (24). Although it varies, the BC mass fraction in fire emissions of $PM_{2.5}$ is generally less than 5% (43). Therefore, no significant trend of BPR can be found in fire-prone areas in the WUS, except in rural and remote areas where an increasing trend exists, likely due to either local wildfire emissions or the transport of smoke particles from the

upwind region (Fig. 4b). In addition, no significant trend in BPR values is found in the southern parts of the Gulf states in the US (Fig. 4b), which may be a result of fire emissions from prescribed burns (44). Overall, however, BPR values increased throughout the US with an average value of 1.82% per year ($p < 0.01$), primarily driven by the increase in the EUS, reflecting a faster decline of other $PM_{2.5}$ components such as sulfate and nitrate concentration as a result of the large reduction in emissions of nitrogen and sulfur oxides dioxide (45-47).

In the WUS, especially in rural areas of California, Nevada, Arizona, and New Mexico, the significant increase in BPR can be explained by the high consistency between the annual mean $PM_{2.5}$ and BC concentrations ($p < 0.01$) and the high correlation of BPR changes with the fire emissions of smoke particles during the last two decades, at a statistically significant level ($p < 0.1$) since 2010 (Fig. S10). Indeed, in the WUS and California, the time series of monthly $PM_{2.5}$ anomaly shows large fluctuations in some individual years associated with large fires, e.g., 2020, 2017, and 2018 (Fig. 4c), when $PM_{2.5}$ concentrations are much higher, with estimates of 46%, 31%, and 30% from wildfires in the WUS, respectively. After these years of heavy wildfire events are removed, the original overall upward trend of $PM_{2.5}$ is replaced by an opposite significant downward trend ($p < 0.01$) of $PM_{2.5}$ pollution in the WUS, especially in California ($p < 0.01$) (Fig. 4d). This attests to the importance of the combined effects of fire emissions and the long-term reduction of anthrophonic emissions in regulating the ambient $PM_{2.5}$ concentration.

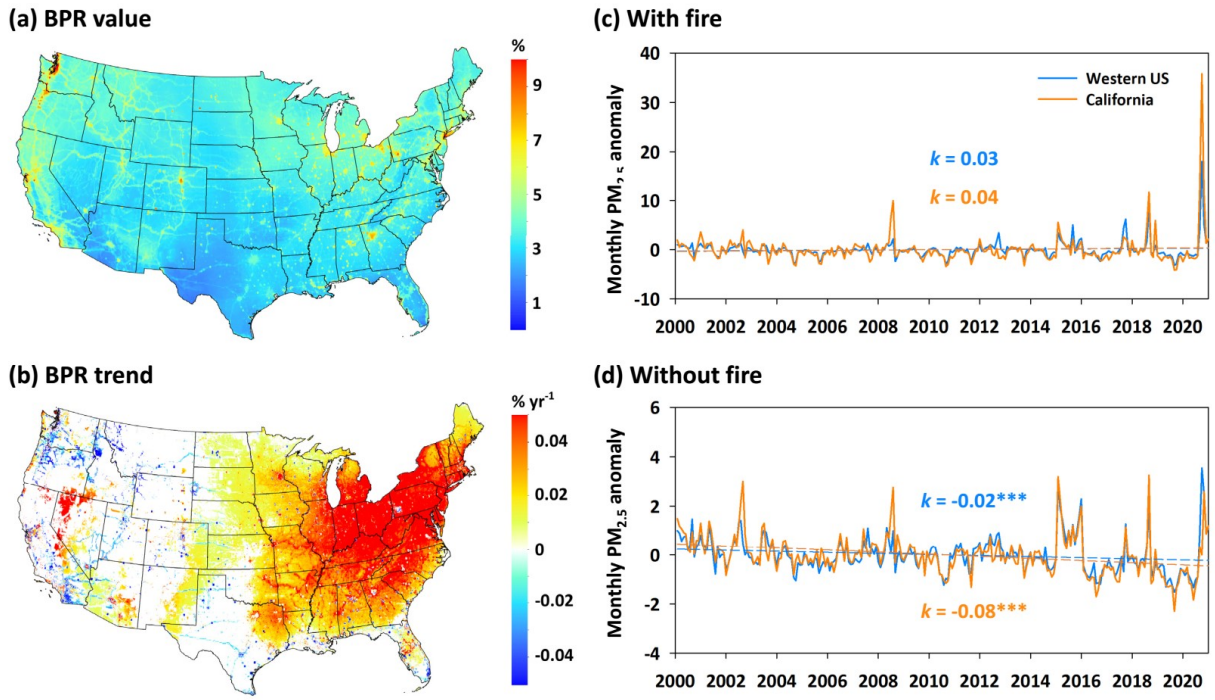

Fig. 4. Spatial distribution of (a) mean (unit: %) and (b) trends (unit: % yr^{-1}) of BC-to-$PM_{2.5}$ ratios (BPR) in summer during the period 2000–2020 across the continental US. Also shown are the time series of monthly $PM_{2.5}$ anomalies (c) before and (d) after removing the years of wildfires from 2000 to 2020 in the western US (blue lines) and California (orange lines), respectively. In (b), only the trends that are significant at the 95% ($p < 0.05$) confidence level are shown. In (c-d), the regression lines are colored by region, and their slope (k, units: μg m^{-3} yr^{-1}) values are given with *, **, and ***, representing trends that are significant at the 90% ($p < 0.1$), 95% ($p < 0.05$), and 99% ($p < 0.01$) confidence levels, respectively.

The toxicity of BC to human health remains uncertain in the literature. Many studies illustrate that BC has a larger relative risk and, therefore, a larger impact on mortality than other $PM_{2.5}$ components (5-8), but some others suggest low confidence (48). As a sensitivity study, we compared estimates of premature deaths under the assumption that BC is no more toxic than and has a similar impact on health as non-BC $PM_{2.5}$ constituents (blue lines in Fig. 3g-i) with deaths calculated assuming larger BC toxicity (orange lines in Fig. 3g-i). We found that the mortality burdens of total $PM_{2.5}$ could be increased by 80-100% and that their trends could have accelerated much more in recent years. This acceleration was distinct in the WUS (slope = 0.73 thousand or 730 per year, $p < 0.05$), resulting in extra loss of life (due to higher toxicity) at the increasing rate of 370 people per year (Fig. 3i), suggesting that the mortality burden is highly related to the variations of BC and that the increasing number and intensity of wildfires in recent years led to

the reversal of the otherwise decreasing trend. Hence, this sensitivity analysis highlights the importance of future studies to accurately define the CRF for BC.

Summary and Conclusion

By combining the long-time-series and high-quality observations of the amounts and compositions of surface $PM_{2.5}$ mass in the US with satellite observations and model reanalysis, we developed a deep-learning approach to generate daily 1-km-resolution, high-quality $PM_{2.5}$ concentrations with full spatial coverage for 21 years (2000–2020) and derived the BC component (often found to be more strongly associated with premature mortality than other aerosol components). The nation-wide $PM_{2.5}$ and BC products estimated in this study agree well with ground-based measurements at highly limited stations. Based on the uniform and fine-resolution data sets, we further investigated the long-term trends of both $PM_{2.5}$ and BC pollution in the US during the last two decades and assessed their impacts on mortality burden at a 1 km fine grid. While $PM_{2.5}$ and BC concentrations have decreased considerably and the mortality burden associated with $PM_{2.5}$ pollution was alleviated overall in 2000–2020 in the continental US, the BC concentration declined at a slower pace and non-uniformly with time. As a result, $PM_{2.5}$ could be relatively more toxic due to the increase of BPR in the US. Furthermore, fire emissions in recent years have led to a national slowdown and a regional reversal in the WUS of the declining trend of mortality burden associated with $PM_{2.5}$ and BC, not only during fire seasons but also at the annual scale. Sensitivity studies underscored the importance of future work to further examine the concentration-response function to BC, especially during fire seasons. The potentially larger toxicity of BC compared to other $PM_{2.5}$ components could further exacerbate the health outcomes associated with the slowdown in the decrease of $PM_{2.5}$ concentration due to fires. The policies to mitigate climate change have co-benefits of reducing not only the impact of heatwaves but also the impact of fire emissions and aerosol composition, especially BC, on public health (49).

Materials and Methods

Big Data. Measurements of surface 24-hour-average $PM_{2.5}$ and BC concentrations were collected daily from the Environmental Protection Agency (EPA) Air Quality System (AQS) and Chemical Speciation Monitoring Network (CSN) and every third day from the Interagency Monitoring of Protected Visual Environments (IMPROVE) (50, 51) at approximately 2740 monitoring stations

from 2000 to 2020 throughout the US. Spatial representation has been improved by integrating the EPA and IMPROVE networks, in which monitors are distributed mainly in urban and rural areas, respectively.

Daily 1-km-resolution Multi-Angle Implementation of Atmospheric Correction (MAIAC) Collection 6 AOD (at 550 nm) products (MCD19A2) retrieved from Moderate Resolution Imaging Spectroradiometer (MODIS) instruments on Terra (~10:30 a.m. local time) and Aqua (~1:30 p.m. local time) satellites since their respective inception (February 25, 2000, and July 4, 2002) to the end of 2020 were employed (52). Also used in the estimates of the surface BC was the Multi-angle Imaging SpectroRadiometer (MISR) Version 23 Level 3 monthly absorbing AOD product (~0.5 degrees) (53). Total aerosol extinction AOD, absorbing AOD (calculated by subtracting scattering AOD from total AOD), black carbon extinction AOD, and the surface mass concentrations of different aerosol components, including BC, organic carbon, dust, sulfate, and sea salt) were collected from MERRA-2 aerosol diagnostics at a horizontal resolution of 0.625° × 0.5° (54). Monthly anthropogenic emissions, including BC, nitrogen oxides, ammonia, sulfur dioxide, and volatile organic compounds, were obtained from the Copernicus Atmosphere Monitoring Service (CAMS) global emission inventories (~0.1 degrees) (55). In addition, monthly smoke emissions from the Fire Energetics and Emissions Research (FEER) database (~0.5 degrees before 2003 and 0.1 degrees after 2003) (56).

Meteorological fields were extracted from ERA5 global reanalysis (~0.1°–0.25° degrees) (57, 58), including the 2 m temperature, precipitation, evaporation, relative humidity, 10 m u-component and v-component of winds, surface pressure, boundary layer height, and surface solar radiation downwards. In addition, the 90 m Shuttle Radar Topography Mission (SRTM) digital elevation model (59), monthly 1 km MODIS normalized difference vegetation index (60) and annual 1 km LandScan^{TM} global population distribution (61) products were also used as inputs in machine learning and prediction. All the auxiliary variables above were aggregated or resampled (using the bidirectional linear interpolation approach) to 0.01° × 0.01° grids (≈ 1 km) to be compatible with the resolution of MAIAC AOD products.

Surface $PM_{2.5}$ and BC estimates with deep learning. A deep learning model was trained by using the aforementioned satellite data and model outputs as features and surface measurements of $PM_{2.5}$ and BC as targets. MAIAC AOD was the primary input to the deep-learning model for $PM_{2.5}$ estimation. Terra and Aqua MODIS AOD values were first integrated using a linear regression model to minimize the difference caused by different observation times and enlarge the spatial coverage (62). In conditions of clouds and snow/ice surfaces and places with satellite swath gaps where MAIAC AOD was missing, AOD values were provided by using MERRA-2 reanalysis. MERRA2 AOD data is generated by assimilating a variety of satellite retrievals (including MODIS) and ground-based observations and has been shown to have accuracy comparable to satellite AOD data in areas with high-density observation networks (e.g., North America and Europe) (63, 64).

To improve the estimates of $PM_{2.5}$, the spatiotemporal autocorrelation and difference in $PM_{2.5}$ were considered in the deep learning, i.e., deep forest (DF) (65), leading to a novel spatiotemporal weighted deep forest (SWDF) model (for details, see SI Text S1). Deep forest is a deep learning model that uses the Cascade structure by including multiple random forests and extremely randomized trees in each middle layer. The final result was determined by integrating the results of all intermediate hidden layers using the Light Gradient Boosting Machine.

Specifically, the model construction included two main steps: we first derived daily $PM_{2.5}$ by training the SWDF model between $PM_{2.5}$ measurements and AOD together with $PM_{2.5}$ components, meteorological fields, anthropogenic emissions of $PM_{2.5}$ precursors, and land-use and population variables. Once $PM_{2.5}$ estimates were made, they were subsequently used as the main predictor in the SWDF model to predict BC mass concentration; additional factors highly associated with BC, e.g., the absorbing AOD and BC AOD, and BC surface mass concentrations and emissions, were also used as inputs in training (for details, see SI Text S1).

For model training, since there were enough data samples for $PM_{2.5}$ every year (i.e., the number of samples, N, ranges from 160,000 to 370,000 per year; total N of all years = 5,931,081), data collected each year from 2000 to 2020 were used to train the SWDF model for that year. Differing from $PM_{2.5}$, all data samples of BC (N = 467,002) collected from the years 2000–2020 were used

380 together to construct the SWDF model for all years since the number of surface BC monitors is
381 smaller than that of $PM_{2.5}$ throughout the US.
382
383 **Mortality Burden Assessment.** The total premature deaths from exposure to ambient $PM_{2.5}$
384 pollution was calculated at each grid box of 1 km in the US for each year from 2000 to 2020 using
385 the concentration-response functions from the GBD 2019 study (28). The GBD framework
386 integrates relative risk with population density, the number of people in each age group, and
387 baseline cause-specific mortality to estimate cases of cause-specific mortality that are attributable
388 to $PM_{2.5}$ (Equation 1). This calculation was carried out separately for mortality from six diseases
389 (i.e., acute lower respiratory infection, chronic obstructive pulmonary disease, ischemic heart
390 disease, lung cancer, stroke (ischemic and hemorrhagic), and diabetes (Type 2)) at 16 different age
391 groups (i.e., children < 5 years old; adults 25-95 at intervals of 5, and > 95 years old), which are
392 then summed to yield total $PM_{2.5}$-attributable mortality:

393 $$MB_{\mathrm{PM}_{2.5}(d,a,y)} = \frac{RR_{d,a,y}-1}{RR_{d,a,y}} \times B_{d,a,y} \times P_y \qquad (1)$$

394 where $MB_{\mathrm{PM}_{2.5}(d,a,y)}$ indicates the mortality burden from the exposure to ambient $PM_{2.5}$, i.e., the
395 number of premature deaths caused by disease *d* for age group *a* in year *y*, and $RR_{d,a,y}$ and $B_{d,a,y}$
396 are the relative risk and baseline mortality of disease *d* for age group *a* in year *y*, which are collected
397 from the disease- and age-specific risk look-up table exceeding the theoretical minimum risk
398 exposure level (TMREL: 2.4–5.9 μg m^{-3}) and from the mortality rate data provided by the GBD
399 2019, respectively. P_y indicates the population in age group *a* in year *y*, where the population data
400 is collected from the LandScan™ global population database at a 1 km resolution.
401
402 The mortality risk of BC to public health is reported to be more harmful (up to ten times higher)
403 than $PM_{2.5}$ (5-8), but no universal concentration-response function for BC is available. Thus, the
404 health burden of BC is assessed by employing the pooled estimate of concentration-response
405 function exposure to long-term BC pollution, i.e., the relative risk per 1 μg m^{-3} increase in BC for
406 all-cause mortality is 1.06 (95% CI: 1.04, 1.09) (5).
407
408 **Acknowledgments.** This work is supported in part by the NASA Applied Science program (grant
409 numbers: 80NSSC19K0191, 80NSSC21K0428, and 80NSSC21K1980) and NASA's MAIA

satellite mission (managed by JPL with contract number 1583456 to the University of Iowa), as well as NOAA's GEO-XO project (grant #: NA21OAR4310249 and NA21OAR4310250) and the NOAA Atmospheric Chemistry, Carbon Cycle and Climate (AC4) program (NA19OAR4310178). C.I. acknowledges support from the NOAA Educational Partnership Program with Minority Serving Institutions (NOAA/EPP/MSI under agreement no. NA16SEC4810006). J.W. also thanks Dr. Jeffrey S. Reid for useful exchanges on fire emission factors of black carbon. The contributions of D.J.D. are carried out at the Jet Propulsion Laboratory, California Institute of Technology, under contract with NASA. The scientific results and conclusions, as well as any views or opinions expressed herein, are those of the author(s) and do not necessarily reflect those of NOAA orthe Department of Commerce.

Data availability. All study data are included in the article and/or SI Appendix. The generated 1-km-resolution $PM_{2.5}$ and BC data of this study are available from the corresponding authors upon request and will be made publicly available once the paper is published. Previously published data were used for this work, and the links for each dataset can be found in the SI Appendix (see SI Text S2).

References

1. Ramanathan V & Feng Y (2009) Air pollution, greenhouse gases and climate change: Global and regional perspectives. *Atmos Environ* 43(1):37-50.
2. Hong CP*, et al.* (2019) Impacts of climate change on future air quality and human health in China. *P Natl Acad Sci USA* 116(35):17193-17200.
3. Bond TC*, et al.* (2013) Bounding the role of black carbon in the climate system: A scientific assessment. *J Geophys Res-Atmos* 118(11):5380-5552.
4. Ramanathan V & Carmichael G (2008) Global and regional climate changes due to black carbon. *Nat Geosci* 1(4):221-227.
5. Janssen NAH*, et al.* (2011) Black Carbon as an Additional Indicator of the Adverse Health Effects of Airborne Particles Compared with PM₁₀ and PM_{2.5}. 119(12):1691-1699.
6. Yang Y*, et al.* (2019) Short-term and long-term exposures to fine particulate matter constituents and health: A systematic review and meta-analysis. *Environ Pollut* 247:874-882.
7. Pond ZA*, et al.* (2021) Cardiopulmonary Mortality and Fine Particulate Air Pollution by Species and Source in a National U.S. Cohort. *Environmental Science & Technology*.
8. Wang Y*, et al.* (2022) Long-term exposure to PM2.5 major components and mortality in the southeastern United States. *Environ Int* 158:106969.
9. Li Y, Henze DK, Jack D, Henderson BH, & Kinney PL (2016) Assessing public health

burden associated with exposure to ambient black carbon in the United States. *Sci Total Environ* 539:515-525.
10. Cleland SE, Serre ML, Rappold AG, & West JJ (2021) Estimating the Acute Health Impacts of Fire-Originated PM(2.5) Exposure During the 2017 California Wildfires: Sensitivity to Choices of Inputs. *GeoHealth* 5(7):e2021GH000414-e002021GH000414.
11. Reid CE*, et al.* (2016) Critical Review of Health Impacts of Wildfire Smoke Exposure. 124(9):1334-1343.
12. Chen H, Samet JM, Bromberg PA, & Tong H (2021) Cardiovascular health impacts of wildfire smoke exposure. *Particle and Fibre Toxicology* 18(1):2.
13. Lee SJ*, et al.* (2012) Comparison of Geostatistical Interpolation and Remote Sensing Techniques for Estimating Long-Term Exposure to Ambient PM2.5 Concentrations across the Continental United States. *Environ Health Persp* 120(12):1727-1732.
14. Beckerman BS*, et al.* (2013) A Hybrid Approach to Estimating National Scale Spatiotemporal Variability of PM2.5 in the Contiguous United States. *Environmental Science & Technology* 47(13):7233-7241.
15. Di Q*, et al.* (2016) Assessing PM2.5 Exposures with High Spatiotemporal Resolution across the Continental United States. *Environmental Science & Technology* 50(9):4712-4721.
16. Hu XF*, et al.* (2017) Estimating PM2.5 Concentrations in the Conterminous United States Using the Random Forest Approach. *Environmental Science & Technology* 51(12):6936-6944.
17. van Donkelaar A, Martin RV, Li C, & Burnett RT (2019) Regional Estimates of Chemical Composition of Fine Particulate Matter Using a Combined Geoscience-Statistical Method with Information from Satellites, Models, and Monitors. *Environmental Science & Technology* 53(5):2595-2611.
18. Di Q*, et al.* (2019) An ensemble-based model of PM2.5 concentration across the contiguous United States with high spatiotemporal resolution. *Environ Int* 130.
19. Park Y*, et al.* (2020) Estimating PM2.5 concentration of the conterminous United States via interpretable convolutional neural networks. *Environ Pollut* 256.
20. Dennison PE, Brewer SC, Arnold JD, & Moritz MA (2014) Large wildfire trends in the western United States, 1984-2011. *Geophys Res Lett* 41(8):2928-2933.
21. Radeloff VC*, et al.* (2018) Rapid growth of the US wildland-urban interface raises wildfire risk. *P Natl Acad Sci USA* 115(13):3314-3319.
22. Zhang L, Lau W, Tao W, & Li Z (2020) Large Wildfires in the Western United States Exacerbated by Tropospheric Drying Linked to a Multi-Decadal Trend in the Expansion of the Hadley Circulation. 47(16):e2020GL087911.
23. Zou Y, Rasch PJ, Wang H, Xie Z, & Zhang R (2021) Increasing large wildfires over the western United States linked to diminishing sea ice in the Arctic. *Nat Commun* 12(1):6048.
24. EPA (2012) EPAUS, Report to Congress on Black Carbon, https://19january2017snapshot.epa.gov/www3/airquality/blackcarbon/2012report/fullreport.pdf.
25. McClure CD & Jaffe DA (2018) US particulate matter air quality improves except in wildfire-prone areas. *Proceedings of the National Academy of Sciences* 115(31):7901.
26. Burnett R*, et al.* (2018) Global estimates of mortality associated with long-term exposure to outdoor fine particulate matter. *P Natl Acad Sci USA* 115(38):9592-9597.
27. Collaborators GCD (2018) GBD 2017 Causes of Death Collaborators. Global, regional,

and national age-sex-specific mortality for 282 causes of death in;195 countries and territories, 1980-2017: a systematic analysis for the Global Burden of Disease Study 2017 (vol 392, pg 1736, 2018). *Lancet* 392(10160):2170-2170.
28. Murray CJL*, et al.* (2020) Global burden of 87 risk factors in 204 countries and territories, 1990-2019: a systematic analysis for the Global Burden of Disease Study 2019. *Lancet* 396(10258):1223-1249.
29. Apte JS, Marshall JD, Cohen AJ, & Brauer M (2015) Addressing Global Mortality from Ambient PM2.5. *Environmental Science & Technology* 49(13):8057-8066.
30. Wang TY*, et al.* (2019) Mortality burdens in California due to air pollution attributable to local and nonlocal emissions. *Environ Int* 133.
31. Aguilera R, Corringham T, Gershunov A, & Benmarhnia T (2021) Wildfire smoke impacts respiratory health more than fine particles from other sources: observational evidence from Southern California. *Nat Commun* 12(1).
32. Smith KR*, et al.* (2009) Public health benefits of strategies to reduce greenhouse-gas emissions: health implications of short-lived greenhouse pollutants. *Lancet* 374(9707):2091-2103.
33. Rodriguez JD, Perez A, & Lozano JA (2010) Sensitivity Analysis of k-Fold Cross Validation in Prediction Error Estimation. *IEEE Transactions on Pattern Analysis and Machine Intelligence* 32(3):569-575.
34. Liang F*, et al.* (2020) The 17-y spatiotemporal trend of PM_{2.5} and its mortality burden in China. 117(41):25601-25608.
35. Chow JC*, et al.* (1993) The dri thermal/optical reflectance carbon analysis system: description, evaluation and applications in U.S. Air quality studies. *Atmospheric Environment. Part A. General Topics* 27(8):1185-1201.
36. Hitzenberger R*, et al.* (2004) Intercomparison of methods to measure the mass concentration of the atmospheric aerosol during INTERCOMP2000—influence of instrumentation and size cuts. *Atmos Environ* 38(38):6467-6476.
37. Li Z*, et al.* (2003) Evaluation of algorithms for fire detection and mapping across North America from satellite. 108(D2).
38. Pu R*, et al.* (2007) Development and analysis of a 12-year daily 1-km forest fire dataset across North America from NOAA/AVHRR data. *Remote Sens Environ* 108(2):198-208.
39. Buechi H, Weber P, Heard S, Cameron D, & Plantinga AJ (2021) Long-term trends in wildfire damages in California %J International Journal of Wildland Fire. 30(10):757-762.
40. Corona-Núñez RO, Li F, & Campo JE (2020) Fires Represent an Important Source of Carbon Emissions in Mexico. 34(12):e2020GB006815.
41. Rios B & Raga G (2019) Smoke emissions from agricultural fires in Mexico and Central America. 13 %J Journal of Applied Remote Sensing(3):036509.
42. Hammer MS*, et al.* (2020) Global Estimates and Long-Term Trends of Fine Particulate Matter Concentrations (1998–2018). *Environmental Science & Technology* 54(13):7879-7890.
43. Prichard SJ*, et al.* (2020) Wildland fire emission factors in North America: synthesis of existing data, measurement needs and management applications. *International Journal of Wildland Fire* 29(2):132-147.
44. Zhang X, Hecobian A, Zheng M, Frank NH, & Weber RJ (2010) Biomass burning impact on PM_{2.5} over the southeastern US during 2007: integrating chemically speciated FRM filter measurements, MODIS fire counts and PMF analysis. *Atmos. Chem.*

Phys. 10(14):6839-6853.
45. Hand JL, Schichtel BA, Pitchford M, Malm WC, & Frank NH (2012) Seasonal composition of remote and urban fine particulate matter in the United States. *J Geophys Res-Atmos* 117.
46. Hand JL, Prenni AJ, Copeland S, Schichtel BA, & Malm WC (2020) Thirty years of the Clean Air Act Amendments: Impacts on haze in remote regions of the United States (1990-2018). *Atmos Environ* 243.
47. Jiang Z*, et al.* (2018) Unexpected slowdown of US pollutant emission reduction in the past decade. *P Natl Acad Sci USA* 115(20):5099-5104.
48. Luben TJ*, et al.* (2017) A systematic review of cardiovascular emergency department visits, hospital admissions and mortality associated with ambient black carbon. *Environ Int* 107:154-162.
49. Ford B*, et al.* (2018) Future Fire Impacts on Smoke Concentrations, Visibility, and Health in the Contiguous United States. 2(8):229-247.
50. Watson JG, Chow JC, Moosmueller H, Green M, & Frank N (1998) Guidance for using continuous monitors in PM2.5 monitoring networks. (United States), p Medium: P; Size: 188 p.
51. Solomon PA*, et al.* (2014) U.S. National PM2.5 Chemical Speciation Monitoring Networks—CSN and IMPROVE: Description of networks. *Journal of the Air & Waste Management Association* 64(12):1410-1438.
52. Lyapustin A, Wang YJ, Korkin S, & Huang D (2018) MODIS Collection 6 MAIAC algorithm. *Atmos Meas Tech* 11(10):5741-5765.
53. Garay MJ*, et al.* (2020) Introducing the 4.4 km spatial resolution Multi-Angle Imaging SpectroRadiometer (MISR) aerosol product. *Atmos. Meas. Tech.* 13(2):593-628.
54. Gelaro R*, et al.* (2017) The Modern-Era Retrospective Analysis for Research and Applications, Version 2 (MERRA-2) %J Journal of Climate. 30(14):5419-5454.
55. Crippa M*, et al.* (2018) Gridded emissions of air pollutants for the period 1970–2012 within EDGAR v4.3.2. *Earth Syst. Sci. Data* 10(4):1987-2013.
56. Ichoku C & Ellison L (2014) Global top-down smoke-aerosol emissions estimation using satellite fire radiative power measurements. *Atmos Chem Phys* 14(13):6643-6667.
57. Hersbach H*, et al.* (2020) The ERA5 global reanalysis. 146(730):1999-2049.
58. Muñoz-Sabater J*, et al.* (2021) ERA5-Land: a state-of-the-art global reanalysis dataset for land applications. *Earth Syst. Sci. Data* 13(9):4349-4383.
59. Farr TG*, et al.* (2007) The Shuttle Radar Topography Mission. 45(2).
60. Didan K (2021) MODIS/Terra Vegetation Indices Monthly L3 Global 1km SIN Grid V061 [Data set]. *NASA EOSDIS Land Processes DAAC*.
61. Bright EA, Coleman PR, Dobson JEJPE, & Sensing R (2000) LandScan: A Global Population Database for Estimating Populations at Risk. 66:849-858.
62. Wei J*, et al.* (2019) Estimating 1-km-resolution PM2.5 concentrations across China using the space-time random forest approach. *Remote Sens Environ* 231.
63. Gueymard CA & Yang D (2020) Worldwide validation of CAMS and MERRA-2 reanalysis aerosol optical depth products using 15 years of AERONET observations. *Atmos Environ* 225:117216.
64. Shi H, Xiao Z, Zhan X, Ma H, & Tian X (2019) Evaluation of MODIS and two reanalysis aerosol optical depth products over AERONET sites. *Atmospheric Research* 220:75-80.
65. Zhou Z-H & Feng J (2017) Deep forest: towards an alternative to deep neural networks. in

Proceedings of the 26th International Joint Conference on Artificial Intelligence (AAAI Press, Melbourne, Australia), pp 3553–3559.